

Transient Responses of a Heterogeneous Spin System to Binomial Pulse Saturation

H. N. YEUNG

Department of Radiology, University of Michigan Medical Center, Ann Arbor, Michigan 48109-0553

Received December 31, 1991; revised June 23, 1992

The transient responses of a heterogeneous spin system to binomial pulses applied at the free-water resonance frequency are obtained by solving the Bloch equations pertaining to such a system modeled by a pair of binary coupled spin baths. Examples of such a solution are given and the validity of the theoretical model is tested by imaging experiments conducted on a phantom consisted of two intact chicken eggs, one raw and the other cooked. © 1993 Academic Press, Inc.

INTRODUCTION

The recent development of magnetization transfer (1-5) on heterogeneous spin systems such as tissues sheds new light on the meaning of relaxation time for these spin-coupled multicomponent systems and the mechanism of how this complex interaction between RF excitation and spin relaxation affects tissue contrast in an imaging experiment. The underlying principle of magnetization-transfer contrast (MTC) is to a large extent based on the cross relaxation between protons in motionally free water and those in the relatively immobile macromolecules. The importance of cross relaxation in tissues signifies that the relaxation of protons in such a system can no longer be treated as single component.

To account for the proton relaxation in biological, or more generally, heterogeneous spin systems, a binary spin-bath model had been invoked (6-10). In such a model, the two spin baths, water (spin bath A) and macromolecular (spin bath B), are considered to be independent thermodynamic systems, and each reaches thermal equilibrium with its own relaxation mechanism. The cross relaxation which describes the magnetization transfer between these two spin baths serves as a link which, by monitoring the NMR signal of the water protons, allows one to pry information from the macromolecules which is otherwise difficult to observe. One of the most powerful methods of achieving this goal is to selectively saturate the macromolecular protons by applying a continuous RF irradiation off the water resonance for a long duration (tens to hundreds of milliseconds) before the water signal is observed. While this off-resonance continuous

irradiation technique is most effective in achieving selective saturation, it is not an easy technique to implement in a clinical MRI system, not to mention the accompanying safety issues inherently involved at high fields. As an alternative to this high-duty-cycle technique, selective B-spin saturation can also be accomplished by a string of periodical binomial pulses applied on resonance (11, 12). Implementation of this pulse saturation scheme is much easier than its continuous irradiation counterpart at the cost of indiscriminate signal loss due to T_2 decay for tissues with short transverse relaxation times (12).

By performing T_1 measurements with continuous off-resonance irradiation and assuming that the B-spin magnetization can be constantly saturated, Grad *et al.* (13) stated that fundamental relaxation rates, namely $1/T_A$ or r_A , the intrinsic spin-lattice relaxation rate of the free-water protons, and the cross-relaxation rate r_X can be measured. By making the same assumption and performing a similar experiment except for the replacement of the continuous RF irradiation by pulse saturation, this author also arrived at the conclusion (14) that the apparent relaxation rate under such conditions approaches the continuous saturation limit of Ref. (13) as the interpulse delay approaches 0. However, in a more extensive study later (15), we showed both in theory and in experiments that the assumption of constant B-spin saturation is in general incorrect and the interpretation of the results in Refs. (13, 14) is valid only under special conditions which do not in general apply to most tissues. In this article, our objective is once again to extend the theory developed for the transient response of the heterogeneous spin systems to continuous saturation (15) to its pulsed analog. To demonstrate the validity and its potential utility in the clinical milieu of the theoretical result, we performed imaging experiments on an egg phantom consisted of two intact chicken eggs, one raw and the other cooked.

THEORY

In Ref. (15), we obtained the transient response of the magnetization under continuous, off-resonance RF irradiation by solving four-component Bloch equations (two trans-

verse components from the immobile protons and the coupled longitudinal components of the two-spin species) by ignoring the effect of the saturating RF on the mobile transverse magnetization. For pulsed saturation, one needs to consider the time development of the longitudinal magnetizations of the binary coupled spin baths in two regimes: one when the saturating RF is turned on and the other when it is off. The effect of a string of binomial RF pulses with pulse duration τ_w separated by an interpulse interval τ_p will be evaluated by solving the Bloch equations pertinent to these two regimes using the end solution of one regime as the initial condition for the next and vice versa.

During the period when the RF pulse with an amplitude ω_1/γ is applied along the x axis of the rotating frame at the resonance frequency of the A spins, the Bloch equations that are pertinent to the binary spin baths once again have four components, although not the same four as in the case of the off-resonance continuous irradiation. In terms of non-dimensional variables, they can be written as

$$\begin{aligned} \frac{dv_A}{d\tau} + \beta_A v_A + \theta_1^n(t)(1 - 2w_A) &= 0 \\ \frac{dv_B}{d\tau} + \beta_B v_B + \theta_1^n(t)(1 - 2w_B) &= 0 \\ \frac{dw_A}{d\tau} + (\alpha_A + \alpha_X)w_A - \alpha_X w_B + \theta_1^n(t) \frac{v_A}{2} &= 0 \\ \frac{dw_B}{d\tau} + \left(\alpha_B + \frac{\alpha_X}{f}\right)w_B - \frac{\alpha_X}{f}w_A + \theta_1^n(t) \frac{v_B}{2} &= 0, \quad [1a] \end{aligned}$$

where $\tau = \omega_1 t$, and v and w are defined by

$$v \equiv \frac{M_v}{M_z^0}, \quad w \equiv \frac{M_z^0 - M_z}{2M_z^0}, \quad [1b]$$

with the others defined as

$$\alpha_\xi = 1/(\omega_1 T_{1\xi}), \quad \beta_\xi = 1/(\omega_1 T_{2\xi}), \quad \xi = A, B,$$

$$\alpha_X = r_X/\omega_1, \quad f = \text{molar ratio of the B spins over A spins.}$$

The function $\theta_1^n(t)$ is a uniamplitude, n th-order binomial function of the RF excitation, i.e., $\theta_1^n(t) \equiv \omega_1^n(t)/|\omega_1|$, where $n = 1, 2, \dots$, specifies the the RF amplitude modulation by the coefficients of x in the binomial expansions $(1 - x)^n$; e.g., for $n = 1, 2$, it is a $1\bar{1}$ and $1\bar{2}1$ pulse, respectively, and so on. The details of the general solution of [1a], very much analogous to the case of off-resonance, continuous excitation (15), which is in turn analogous to Torry's transient solution to the original Bloch equations (16), are given in the Appendix. If we let the column vector $\mathbf{X} \equiv \{v_A, v_B, w_A, w_B\}^T$ be the solution of [1a], then the general solution $\mathbf{X}(\tau)$ is

formally identical to that of the case of the continuous saturation (15), i.e.,

$$\begin{aligned} \mathbf{X}(\tau) &= \mathbf{A}e^{-a\tau} + \mathbf{B}e^{-b\tau} + \mathbf{C}e^{-c\tau} \cos(s\tau) \\ &\quad + \frac{\mathbf{D}}{s} e^{-c\tau} \sin(s\tau) + \mathbf{E}, \quad [2] \end{aligned}$$

but with a totally different set of time constants a, b, c , and s and a different set of coefficient vectors $\mathbf{A}, \mathbf{B}, \mathbf{C}, \mathbf{D}$, and \mathbf{E} as well. The column vector \mathbf{E} in [2] represents the steady-state solution while the other four terms represent the transient responses of the spin system. As in the case of continuous saturation, the constants a, b, c , and s along with \mathbf{E} are all independent of the initial conditions of how the spin system is prepared. The vectors $\mathbf{A}, \mathbf{B}, \mathbf{C}$, and \mathbf{D} , on the other hand, depend on the initial conditions which are given by the column vectors $\mathbf{X}(0)$ and its time derivative $\mathbf{X}'(0)$. The expressions of all these quantities are also given in the Appendix.

In the absence of RF field, only the longitudinal components of the Bloch equations of the spin bath in Eq. [1a] need to be considered. By setting $\theta_1^n(t)$ to zero, the last two component equations in [1a] can be written in matrix form as

$$\begin{aligned} \frac{d\tilde{\mathbf{U}}}{dt} &= -\mathbf{P}\tilde{\mathbf{U}}; \quad \tilde{\mathbf{U}} = \begin{bmatrix} w_A \\ w_B \end{bmatrix}, \\ \mathbf{P} &= \begin{bmatrix} r_A + r_X & -r_X \\ -r_X/f & r_B + r_X/f \end{bmatrix}. \quad [3] \end{aligned}$$

To solve [3], we seek a transformation to diagonalize the relaxation matrix \mathbf{P} . This is tantamount to finding a set of eigenvectors which correspond to the eigenvalues of \mathbf{P} :

$$\begin{aligned} \lambda_{\pm} &= \frac{1}{2} \left\{ r_A + r_B + r_X \left(1 + \frac{1}{f} \right) \right\} \\ &\quad \pm \frac{1}{2} \left\{ \sqrt{\left[r_A - r_B + r_X \left(1 - \frac{1}{f} \right) \right]^2 + 4r_X^2} \right\}. \quad [4] \end{aligned}$$

If we let \mathbf{Q} be a transformation such that $\mathbf{Q}^{-1}\mathbf{P}\mathbf{Q} = \mathbf{\Lambda}$, $\Lambda_{ij} = \lambda_i \delta_{ij}$, then we can write

$$\tilde{\mathbf{U}}(t) = \mathbf{R}(t)\tilde{\mathbf{U}}(0), \quad [5]$$

where

$$\begin{aligned} \mathbf{R}(t) &= \mathbf{Q}e^{-\mathbf{\Lambda}t}\mathbf{Q}^{-1} = \frac{1}{\lambda_- - \lambda_+} \left\{ \begin{bmatrix} \rho_{AA}^+ & \rho_{AB}^+ \\ \rho_{BA}^+ & \rho_{BB}^+ \end{bmatrix} e^{-\lambda_+ t} \right. \\ &\quad \left. + \begin{bmatrix} \rho_{AA}^- & \rho_{AB}^- \\ \rho_{BA}^- & \rho_{BB}^- \end{bmatrix} e^{-\lambda_- t} \right\} \quad [6] \end{aligned}$$

$$\begin{aligned} \text{with } \rho_{\bar{A}A}^{\pm} &= \mp(r_A + r_X) \pm \lambda_{\mp}, \quad \rho_{\bar{A}B}^{\pm} = \pm r_X, \\ \rho_{\bar{B}A}^{\pm} &= \pm r_X/f, \quad \rho_{\bar{B}B}^{\pm} = \pm(r_A + r_X) \mp \lambda_{\pm} = \rho_{\bar{A}A}^{\mp}. \end{aligned}$$

The solution of the mobile magnetization in this RF-free period is given by

$$w_A(t) = g_A(t)w_A(0) + g_B(t)w_B(0), \quad [7]$$

where

$$g_A(t) = \frac{(r_W + r_X)(e^{-\lambda_+ t} - e^{-\lambda_- t}) - (\lambda_- e^{-\lambda_+ t} - \lambda_+ e^{-\lambda_- t})}{\lambda_- - \lambda_+} \quad [8a]$$

$$g_B(t) = \frac{r_X(e^{-\lambda_+ t} - e^{-\lambda_- t})}{\lambda_- - \lambda_+}. \quad [8b]$$

The time decay of $w_A(t)$, according to [7], will depend on the boundary conditions, $w_A(0)$ and $w_B(0)$, prescribed by the pulse sequence of the measurement. For a conventional inversion-recovery sequence without saturation, $w_A(0) = w_B(0) = 1$, and

$$\begin{aligned} W_{ns}(t) &= g_A(t) + g_B(t) \\ &= \frac{-(r_A - \lambda_+)e^{-\lambda_+ t} + (r_A - \lambda_-)e^{-\lambda_- t}}{\lambda_- - \lambda_+}. \quad [9] \end{aligned}$$

From the above expression, we note that the decay of $W_{ns}(t)$ is in general not monoexponential, a well-known fact which had been pointed out in many previous studies (9, 17, 18). This biexponentiality is especially pronounced at the initial part of the decay. At later times, as the fast-decaying components die down, the decay becomes exponential with an apparent relaxation rate constant λ_- .

To evaluate the responses of the spin system to a pulse saturation burst which consists of a train of binomial pulses, with pulse duration τ_w and interpulse delay τ_p , one starts with an initial magnetization and obtains a solution in the pulse-on regime $\mathbf{X}(\tau_w)$ according to [2]. One then uses the last two components in $\mathbf{X}(\tau_w)$ as the initial vector for the solution of the pulse-off regime; i.e., $\mathbf{U}(\tau_w) = \{X_3(\tau_w), X_4(\tau_w)\}^T$. After the solution vector $\mathbf{U}(\tau_w + \tau_p)$ is obtained from [5] and [6], it is used in turn as part of the initial condition for the ensuing pulse-on regime; i.e., $\mathbf{X}(\tau_w + \tau_p) = \{X_1(\tau_w)e^{-\beta_A \tau_p}, X_2(\tau_w)e^{-\beta_B \tau_p}, U_1(\tau_w + \tau_p), U_2(\tau_w + \tau_p)\}^T$. The time evolution of the spin system can be carried on by this cyclic process indefinitely until the steady state is reached after a sufficient number of cycles. At steady state, if we let \mathbf{X}_{ss} be the state vector at the end of the free-induction period and \mathbf{X}'_{ss} be that immediately following the binomial pulse, then

$$X_{1ss} = X'_{1ss}e^{-\beta_A \tau_p}, \quad X_{2ss} = X'_{2ss}e^{-\beta_B \tau_p}$$

$$X_{3ss} = R_{11}(\tau_p)X'_{3ss} + R_{12}(\tau_p)X'_{4ss},$$

$$X_{4ss} = R_{21}(\tau_p)X'_{3ss} + R_{22}(\tau_p)X'_{4ss},$$

where $\mathbf{X}'_{ss} = \mathbf{X}(\tau_w)$, with the initial vector $\mathbf{X}(0) = \mathbf{X}_{ss}$.

NUMERICAL EVALUATIONS

To illustrate concretely the responses of a heterogeneous system to the application of a train of binomial pulses, we perform numerical calculations using, unless specified otherwise, a parameter set of the cooked egg white (see under Results and Discussion for its derivation) to illustrate the important features of the binomial pulse saturation. To illustrate the effect of cross relaxation on transient response in the calculation, the cross-relaxation rate r_X is allowed to vary hypothetically from zero to five times its realistic value. Also varied are the pulse sequence parameters that are pertinent to the transient responses. These are the RF field strength ω_1 , the pulse duration τ_w , and the delay between the binomial pulses τ_p .

The first example, shown in Fig. 1, shows the transient behavior of the two longitudinal components during a 2.5 ms 11 pulse and the ensuing free-induction period, $\tau_p = 15$ ms. In this example, r_X is inflated to five times its realistic value (3.6 s^{-1} ; see below) to dramatize the effect of the cross relaxation. The response curves illustrate the main objective of the binomial pulse: to saturate the B spins while leaving the A spins relatively unscathed. Note also that during the

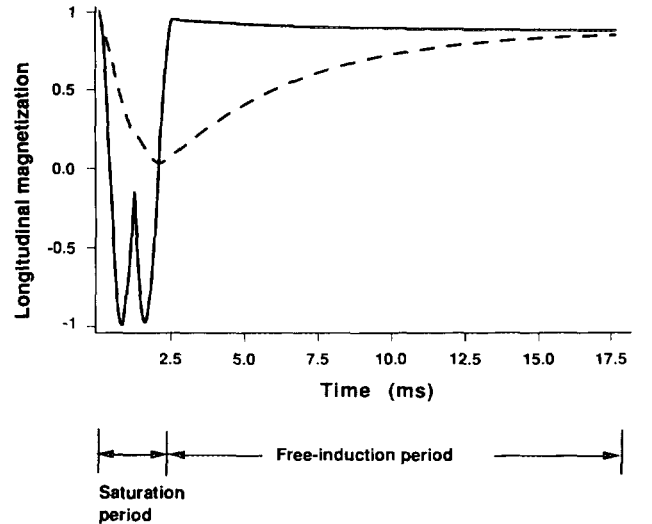


FIG. 1. Transient response to a binomial pulse and its subsequent delay in a hypothetical system which has the same model parameters as the cooked egg white except for the cross-relaxation rate r_X , which is inflated to five times its realistic value. Solid line, M_z of the free-water component; broken line, M_z of the macromolecular component.

free-induction period, M_{ZB} recovers relatively rapidly while M_{ZA} continues to decline, although only sparingly. This result can be readily rationalized by the parameter set used in which $r_X > 1/T_{1A}$, $1/T_{1B}$ and $f \ll 1$. The second example, shown in Fig. 2, illustrates the cumulative effect of the pulse saturation burst on the transient development of the spin system. In this and all the subsequent plots, only the endpoints of the pulse and free-induction intervals will be used. By connecting them sequentially, the response curves show a zig-zag-like pattern. Figure 2a shows both M_{ZA} (solid line) and M_{ZB} (broken line) at the various end intervals during the time course of the pulse saturation burst. The decay shown in the A component is the result of two effects: cross relaxation and T_2 decay. To assess the separate contribution of these two effects, we make the same plots in Fig. 2b, this time only for the A-spin component, at different τ_p values, with the cross-relaxation effect switched on (solid lines) and off (broken lines). Thus the solid lines show the combined

effects while the broken lines show only the T_2 decay. Finally, in Fig. 2c, the same plots in Fig. 2b are repeated except for the fact that the pulse duration τ_w is halved while the RF field strength ω_1 is raised by a factor of 1.5. This illustrates that the T_2 effect can be decreased relative to the cross-relaxation effect by using shorter but stronger binomial pulses and a longer interpulse interval.

METHODS AND MATERIALS

To empirically verify the validity of the theoretical model, we once again follow the practice of Ref. (15) and use cooked egg white as an example by performing experiments on a phantom which consists of two intact chicken eggs, one raw and the other cooked in boiling water for 20 minutes. Three sets of 2D single-slice imaging pulse sequences were used in these experiments:

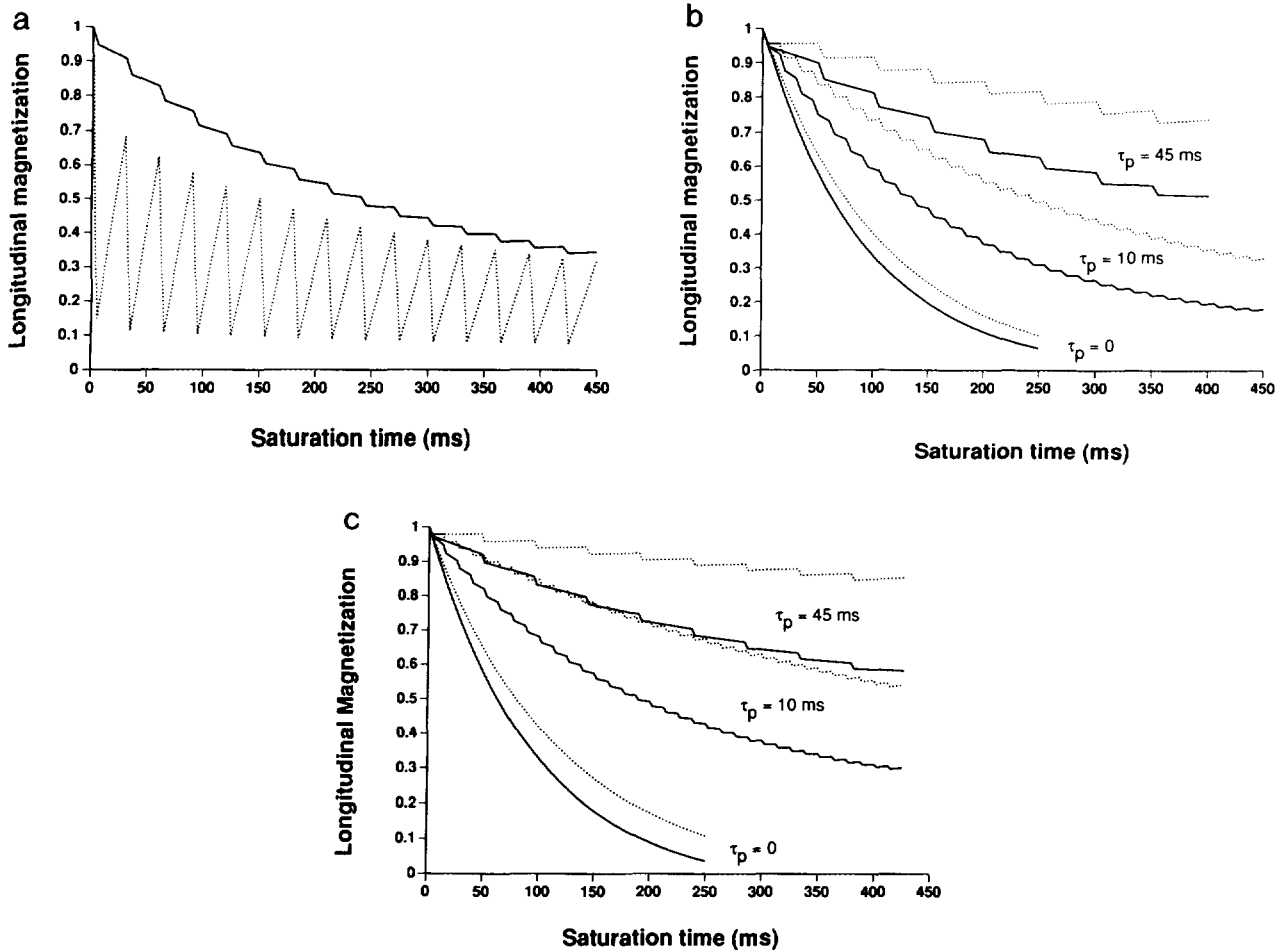


FIG. 2. The zig-zag lines are the time courses of the M_z responses to pulse saturation resulting from connecting the sequential end-interval solutions to a train of binomial pulses alternated with free delays τ_p . Unless specified otherwise, the model parameters are the same as those of the cooked egg white and the RF parameters are $\tau_w = 5$ ms, $\omega_1 = 2440$ rad/s, and τ_p varies from 0 to 45 ms. (a) $\tau_p = 25$ ms. Solid line, M_z of the free-water component; broken line, M_z of the macromolecular component. (b) M_z responses of the free-water component at τ_p of 0, 10, and 45 ms, respectively. Solid line, $r_X = 3.6$ s $^{-1}$; broken line, $r_X = 0$. (c) Same as (b) except that the pulse width of the binomial pulse τ_w is halved and the RF field strength ω_1 is increased by 50%.

(a) T_2 imaging sequence using a 4-point, CPMG multiple-echo technique.

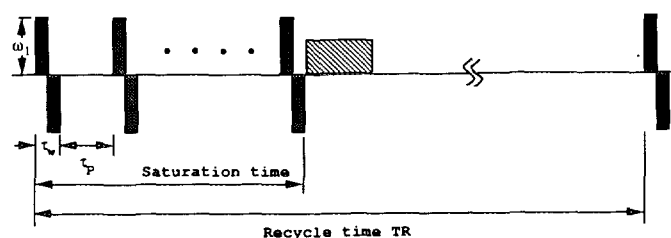
(b) T_1 imaging sequence using a 16-point imaging version (19, 20) of the Look-and-Locker (21), one-shot IR technique.

(c) Standard spin-echo imaging sequences preceded by periodic pulse presaturation (Fig. 3) with $1\bar{1}$ binomial pulses of various pulse strengths and widths. Also varied are the interpulse timing τ_p and the total number of pulses N which determined the time of sampling of the transient decay.

The experiments were performed in a 0.5 T whole-body imaging system manufactured by Picker International (Height, Ohio). The imaging parameters were TR = 2 s; TE = 30, 60, 90, and 120 ms in (a), 13 ms in (b) (since the imaging sequence for this set uses a gradient echo, the TE here is the gradient-refocused time), and 20 ms in (c); number of phase-encoding data lines = 128; number of signal accumulations = 4; field of view = 15 cm; and slice thickness = 7.5 mm. The tip angle of the slice-selective "read" RF pulse is 90° in (c) and 10° in (b). In (b), the interpulse delay between the read pulses is 104 ms and the inversion pulse used is a $90_x^\circ - 180_y^\circ - 90_x^\circ$ nonselective composite pulse.

RESULTS AND DISCUSSION

The results of the measured proton relaxation times for egg white of the two intact chicken eggs are summarized in Table 1. The results of the transient decay of the longitudinal egg white magnetization under different saturation conditions as determined in sequence (c) are summarized in Table 2. To interpret the data in Table 2, our goal is to find a set of parameters, namely $\{T_{1A}, T_{1B}, T_{2A}, T_{2B}, r_X, f\}$, to fit all the data in Table 2. While it is possible to use sophisticated means of linear programming or optimization to achieve this goal, it is, however, much easier and perhaps more gratifying to rely on physical intuition. Our strategy is simply to




 = Events of standard imaging sequence

FIG. 3. Pulse sequence used to obtain *in vivo* transient responses to binomial pulse saturation. The RF duty cycle and saturation time are varied by the adjustment of the pulse width τ_w , the RF amplitude ω_1 , and the interpulse delay τ_p .

TABLE 1
Apparent T_1 and T_2 of Raw and Cooked Egg White in an Intact Chicken Egg

Egg white	T_1 (ms)	T_2 (ms)
Raw	1133 ± 117	199 ± 24
Cooked	786 ± 62	60 ± 8

assume a set of parameter values based on empirical reasoning and then calculate the transient responses according to theory developed above and compare them to the experimental results in Table 2. We first assume that, in the raw egg white (REW), the egg albumin molecules are too small to be effective in bringing about cross relaxation between the free-water and protein components. As a consequence, it is reasonable to assume that the measured apparent T_1 value of the REW is the intrinsic T_1 of the free-water component which remains the same after the egg is cooked. So for the cooked egg white (CEW), we establish, from Table 1, $r_A = 1/T_{1REW} = 0.88 \text{ s}^{-1}$, $T_{2A} = 60 \text{ ms}$. The parameters T_{2B} , r_X , and f have been previously determined (15) empirically at 2.0 T. Among these parameters, f is a constant and the frequency dependences of T_{2B} and r_X , although not known precisely, are believed to be small for the frequency range that concerns us here (22). Thus, it is a good approximation to use the 2.0 T values of these three parameters without modification: $f = 0.09$, $T_{2B} = 60 \mu\text{s}$, $r_X = 3.6 \text{ s}^{-1}$. Finally, r_B or $1/T_{1B}$ is fixed by Eq. [4] for the given r_A , r_X , f specified above and $\lambda = 1/T_{1CEW}$ or 1.27 s^{-1} from Table 1. Solving r_B from [4] yields a value of 6.12 s^{-1} .

Using the parameter set established above, the transient responses of the longitudinal magnetization of the free-water component in egg white under pulse saturation are evaluated under the same conditions as those used in the pulse sequence in Fig. 3 as described in (c). The results of these calculations along with the experimental data points in Table 2 are plotted in Fig. 4. It is interesting to note that both the calculations and the experimental data show very similar responses for the cooked egg white (the two curves around the data points symbolized by \blacktriangle 's \blacklozenge 's) when the saturation pulse burst has a similar RF duty cycle. Given the fact that there is no "fitting" in this comparison between theory and experiment, the agreement, while not perfect, is good enough to justify the adequacy of the spin-bath model, if not also the parameter set, for the heterogeneous spin systems typified by the egg white or other animal tissues.

To conclude, we have extended the analytical, albeit implicit, solution of the transient responses of a heterogeneous spin system to RF saturation from CW to a train of periodic binomial pulses using a binary spin-bath model. We have also demonstrated the validity of such a model for the description of the spin system by showing good agreement be-

TABLE 2
Time Course of Signal Intensity of the Egg Phantom under Periodic Pulse Saturation

		Saturation time (ms)							
		0	65	125	185	245	305	365	425
		$\tau_p = 10 \text{ ms}, \tau_w = 5 \text{ ms}, \omega_1 = 2440 \text{ rad/s}$							
Raw egg white									
Signal intensity	1309	1138	1072	1017	971	929	882	849	816
Ratio(sat/no sat) ^a	1.0	0.880	0.839	0.807	0.780	0.758	0.731	0.716	
Cooked egg white									
Signal intensity	1272	860	649	503	405	331	279	241	211
Ratio(sat/no sat) ^a	1.0	0.681	0.518	0.404	0.328	0.271	0.231	0.202	
		$\tau_p = 25 \text{ ms}, \tau_w = 5 \text{ ms}, \omega_1 = 2440 \text{ rad/s}$							
Raw egg white									
Signal intensity	1309	1212	1162	1126	1083	1039	1000	965	930
Ratio(sat/no sat) ^a	1.0	0.937	0.915	0.905	0.891	0.876	0.861	0.846	0.831
Cooked egg white									
Signal intensity	1272	982	777	636	541	480	425	370	315
Ratio(sat/no sat) ^a	1.0	0.772	0.610	0.500	0.425	0.370	0.315	0.260	0.205
		$\tau_p = 15 \text{ ms}, \tau_w = 2.5 \text{ ms}, \omega_1 = 3660 \text{ rad/s}$							
Raw egg white									
Signal intensity	1222	1125	1092	1065	1042	996	957	933	913
Ratio(sat/no sat) ^a	1.0	0.927	0.909	0.896	0.887	0.858	0.835	0.826	0.817
Cooked egg white									
Signal intensity	1112	932	786	667	571	497	437	382	327
Ratio(sat/no sat) ^a	1.0	0.838	0.707	0.600	0.514	0.447	0.393	0.343	0.293

^a Rescaled to account for differences in recovery time for each time point.

tween results obtained from experiments and theoretical calculations based on this model. By knowing the general solution to the model equations, we hope that it will enable us to embark on the attractive, though challenging, task of determining and cataloging the model parameters for such landmark animal tissues as brain white matter, muscle, and liver and their field dependence through empirical means. It is our belief that the knowledge of these parameters is indispensable to the fundamental understanding of how tissue contrast in general and MTC in particular affect NMR imaging experiments.

APPENDIX

The method given here for the general solution of the coupled equations in [1a] is analogous to the one we used for the solution of the case of continuous off-resonance RF saturation. This in turn followed from the procedure given by Torrey (16) in his Appendix for the general solution of the Bloch equations. For this reason, only the main steps will be given.

The Laplace transforms of Eq. [1a] in the text are

$$(p + \beta_A)\tilde{v}_A - 2\theta(t)\tilde{w}_A = v_{A0} - \frac{\theta_1^n(\tau')}{p},$$

$$\tau' = \text{mod}(\tau, \tau_w + \tau_p), \tau' \leq \tau_w \quad [\text{A1a}]$$

$$(p + \beta_B)\tilde{v}_B - 2\theta(\tau')\tilde{w}_B = v_{B0} - \frac{\theta_1^n(\tau')}{p} \quad [\text{A1b}]$$

$$\theta_1^n(\tau') \frac{\tilde{v}_A}{2} + (p + \alpha_A + \alpha_X)\tilde{w}_A - \alpha_X \tilde{w}_B = w_{A0} \quad [\text{A1c}]$$

$$\theta_1^n(\tau') \frac{\tilde{v}_B}{2} - \frac{\alpha_X}{f} \tilde{w}_A + \left(p + \frac{\alpha_X}{f} + \alpha_B\right)\tilde{w}_B = w_{B0}, \quad [\text{A1d}]$$

where \tilde{v}_A , \tilde{v}_B , \tilde{w}_B , and \tilde{w}_A are the transforms and v_{A0} , v_{B0} , w_{A0} , and w_{B0} the initial values of v_A , v_B , w_A , and w_B , respectively. If we write $\tilde{\mathbf{X}} = \{\tilde{v}_A, \tilde{v}_B, \tilde{w}_B, \tilde{w}_A\}^T$. The solutions of [A1] can be given as

$$\tilde{\mathbf{X}} = \frac{\mathbf{g}}{p\Delta(p)}, \quad [\text{A2}]$$

where the components of vector \mathbf{g} are

$$\begin{aligned}
g_1(\tau', p) \equiv & \left\{ \beta_B \alpha_A \frac{\alpha_X}{f} + (\alpha_A + \alpha_X)(1 + \alpha_B \beta_B) \right. \\
& + p \left[\frac{\alpha_X}{f} (\alpha_A + \beta_A) + 1 + \alpha_B (\alpha_A + \alpha_X) \right. \\
& \left. \left. + \beta_B (\alpha_A + \alpha_B + \alpha_X) \right] + p^2 [\alpha_A + \alpha_B + \alpha_X (1 + 1/f) \right. \\
& \left. + \beta_B] + p^3 \left\{ p v_{A0} - \theta_1^n(\tau') - \alpha_X [p v_{B0} - \theta_1^n(\tau')] \right. \right. \\
& \left. \left. + 2\theta_1^n(\tau') (\alpha_B + \alpha_X/f) \beta_B + 1 + p (\alpha_B + \alpha_X/f + \beta_B) \right. \right. \\
& \left. \left. + p^2 \right\} p w_{A0} + 2\theta_1^n(\tau') \alpha_X (p + \beta_B) p w_{B0} \quad [\text{A3a}]
\end{aligned}$$

$$\begin{aligned}
g_2(\tau', p) \equiv & \left\{ \left(\frac{\alpha_X}{f} + \alpha_B \right) (1 + \alpha_A \beta_A) + \alpha_B \alpha_X \beta_A \right. \\
& + p \left[\frac{\alpha_X}{f} (\alpha_A + \beta_A) + 1 + \alpha_B (\alpha_A + \alpha_X) \right. \\
& \left. + \beta_A (\alpha_A + \alpha_B + \alpha_X) \right] + p^2 [\alpha_A + \alpha_B + \alpha_X (1 + 1/f) \\
& \left. + \beta_A] + p^3 \left\{ [p v_{B0} - \theta_1^n(\tau')] - \frac{\alpha_X}{f} [p v_{A0} - \theta_1^n(\tau')] \right. \right. \\
& \left. \left. - \frac{\alpha_X}{f} [p v_{A0} - \theta_1^n(\tau')] + 2\theta_2^n(\tau') \right\} \right. \\
& \times \left\{ \frac{\alpha_X}{f} (p + \beta_A) p w_{A0} + (p + \beta_A) (\alpha_A + \alpha_X) \right. \\
& \left. \left. + \beta_A p + p^2 \right\} p w_{B0} \quad [\text{A3b}]
\end{aligned}$$

$$\begin{aligned}
g_3(\tau', p) \equiv & -\frac{\alpha_X}{2} (p + \beta_A) [p \theta_1^n(\tau') v_{B0} - 1] \\
& + \left\{ \beta_B \left(\alpha_B + \frac{\alpha_X}{f} \right) + 1 + \left(\alpha_B + \frac{\alpha_X}{f} + \beta_B \right) p + p^2 \right\} \\
& \times \left\{ (p + \beta_A) p w_{A0} - \frac{1}{2} [\theta_1^n(\tau') p v_{A0} - 1] \right\} \\
& + (p + \beta_A) (p + \beta_B) \alpha_X p w_{B0} \quad [\text{A3c}]
\end{aligned}$$

$$\begin{aligned}
g_4(\tau', p) \equiv & [1 + \beta_A (\alpha_A + \alpha_X) + p (\alpha_A + \alpha_X + \beta_A) \\
& + p^2] \left[-\frac{\theta_1^n(\tau') p v_{B0} - 1}{2} + (p + \beta_B) p w_{B0} \right] + \frac{\alpha_X}{f} \\
& \times (p + \beta_B) \left\{ (p + \beta_A) p w_{A0} - \frac{1}{2} [\theta_1^n(\tau') p v_{A0} - 1] \right\}; \quad [\text{A3d}]
\end{aligned}$$

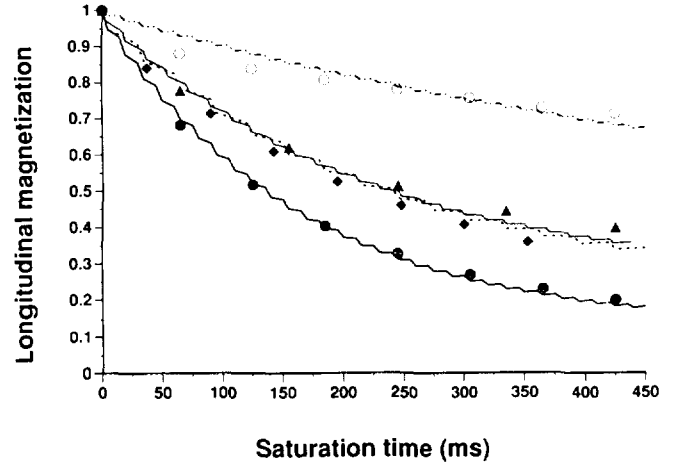


FIG. 4 Comparison of transient M_z decay of egg whites evaluated by the theoretical model to experimental data:

RF parameters (time in ms, ω_1 in rad/s)	Type of egg white	Legends for	
		Theoretical curves	Data
$\tau_w = 5, \tau_p = 10, \omega_1 = 2440$	Raw	(---)	○
$\tau_w = 5, \tau_p = 10, \omega_1 = 2440$	Cooked	(—)	●
$\tau_w = 5, \tau_p = 25, \omega_1 = 2440$	Cooked	(- - - -)	▲
$\tau_w = 2.5, \tau_p = 15, \omega_1 = 3660$	Cooked	(.....)	◆

where

$$\begin{aligned}
\Delta(p) = & p^4 + p^3 [\alpha_A + \alpha_B + \alpha_X (1 + 1/f) + \beta_A + \beta_B] \\
& + p^2 \left\{ \frac{\alpha_A \alpha_X}{f} + 2 + \alpha_B (\alpha_A + \alpha_X) + (\beta_A + \beta_B) \right. \\
& \times [\alpha_A + \alpha_B + \alpha_X (1 + 1/f)] + \beta_A \beta_B \left. \right\} + p \left\{ (1 + \beta_A \beta_B) \right. \\
& \times [\alpha_A + \alpha_B + \alpha_X (1 + 1/f)] + (\beta_A + \beta_B) \\
& \times \left[1 + \alpha_B (\alpha_A + \alpha_X) + \frac{\alpha_A \alpha_X}{f} \right] \left. \right\} + 1 + \frac{\beta_B \alpha_X}{f} (1 + \alpha_A \beta_A) \\
& + \beta_A (\alpha_A + \alpha_X) (1 + \alpha_B \beta_B) + \alpha_B \beta_B \quad [\text{A4}]
\end{aligned}$$

is the determinant of the coefficients in [A1]. Physical reality dictates that the quartic equation $\Delta(p) = 0$ have at least two negative roots. Let these roots be $-a, -b$; then $\Delta(p)$ can be factored into

$$\Delta(p) = (p + a)(p + b)\{(p + c)^2 + s^2\}. \quad [\text{A5}]$$

Equation [A2] can now be expanded in partial fractions:

$$\tilde{X}(p) = \frac{\mathbf{A}}{p + a} + \frac{\mathbf{B}}{p + b} + \frac{\mathbf{C}p + \mathbf{D}}{(p + c)^2 + s^2} + \frac{\mathbf{E}}{p}. \quad [\text{A6}]$$

The inverse Laplace transform of [A6] yields the desired general solution:

$$\mathbf{X}(\tau) = \mathbf{A}e^{-a\tau} + \mathbf{B}e^{-b\tau} + \mathbf{C}e^{-c\tau}\cos(s\tau) + \frac{\mathbf{D}}{s}e^{-c\tau}\sin(s\tau) + \mathbf{E}. \quad [\text{A7}]$$

It is clear from [A7] that \mathbf{E} yields the steady-state solutions while \mathbf{A} , \mathbf{B} , \mathbf{C} , and \mathbf{D} determine the transient behavior of magnetization. The constants c and s are determined by equating coefficients of the terms in same powers in p of the identity

$$\Delta(p) \equiv (p+a)(p+b)\{(p+c)^2 + s^2\}$$

or, from [A3] we obtain

$$c = \frac{1}{2} \{ \alpha_B + \alpha_A + \alpha_X(1 + 1/f) + (\beta_A + \beta_B) - (a + b) \} \quad [\text{A8a}]$$

$$s = \{ [\beta_A(\alpha_A + \alpha_X)(1 + \alpha_B\beta_B) + \alpha_B\beta_B + (\beta_B\alpha_X/f)(1 + \alpha_A\beta_A)/ab - c^2]^{1/2} \}. \quad [\text{A8b}]$$

The coefficient vectors \mathbf{A} , \mathbf{B} , and \mathbf{E} are given, from [A6] and [A4], by the relations

$$\mathbf{E} = \lim_{p \rightarrow 0} p\tilde{\mathbf{X}}(p) = \frac{\mathbf{g}(0)}{\Delta(0)} \quad [\text{A9}]$$

$$\mathbf{A} = \lim_{p \rightarrow a} (p+a)\tilde{\mathbf{X}}(p) = \frac{-\mathbf{g}(-a)}{a(b-a)\{(c-a)^2 + s^2\}} \quad [\text{A10}]$$

$$\mathbf{B} = \lim_{p \rightarrow b} (p+b)\tilde{\mathbf{X}}(p) = \frac{-\mathbf{g}(-b)}{b(a-b)\{(c-b)^2 + s^2\}}. \quad [\text{A11}]$$

Once \mathbf{A} , \mathbf{B} , and \mathbf{E} are fixed, the vectors \mathbf{C} and \mathbf{D} are readily obtainable from the initial conditions on \mathbf{X} and on its time derivative; i.e.,

$$\mathbf{C} = \mathbf{X}(0) - \mathbf{A} - \mathbf{B} - \mathbf{E} \quad \text{and}$$

$$\mathbf{D} = a\mathbf{A} + b\mathbf{B} + c\mathbf{C} + \mathbf{X}'(0). \quad [\text{A12}]$$

REFERENCES

1. S. D. Wolff and R. S. Balaban, *Magn. Reson. Med.* **10**, 135 (1989).
2. J. Eng, T. L. Ceckler, and R. S. Balaban, *Magn. Reson. Med.* **17**, 304 (1991).
3. J. Grad, D. Mendelson, F. Hyder, and R. G. Bryant, *Magn. Reson. Med.* **17**, 452 (1991).
4. S. D. Wolff and R. S. Balaban, *Radiology* **179**, 133 (1991).
5. S. D. Wolff, S. Chesnick, J. A. Frank, K. O. Lim, and R. S. Balaban, *Radiology* **179**, 623 (1991).
6. S. H. Koenig, R. G. Bryant, K. Hallenga, and G. A. Jacob, *Biochemistry* **17**, 4348 (1978).
7. H. T. Edzes and E. T. Samulski, *J. Magn. Reson.* **31**, 207 (1978).
8. H. T. Edzes and E. T. Samulski, *Nature* **265**, 521 (1977).
9. B. M. Fung and T. W. McGaughey, *J. Magn. Reson.* **39**, 413 (1980).
10. J. Grad and R. G. Bryant, *J. Magn. Reson.* **90**, 1 (1990).
11. B. Hu, D. Nishimura, and A. Macovski, Abstracts of the Society of Magnetic Resonance in Medicine, 9th Annual Meeting, New York, p. 352, 1990.
12. H. N. Yeung and A. M. Aisen, *Radiology* **183**, 209 (1992).
13. J. Grad, D. Mendelson, F. Hyder, and R. G. Bryant, *J. Magn. Reson.* **86**, 416 (1990).
14. H. N. Yeung, Abstracts of the Society of Magnetic Resonance in Medicine, 10th Annual Meeting, San Francisco, p. 174, 1991.
15. H. N. Yeung and S. D. Swanson, *J. Magn. Reson.* **99**, 466 (1992).
16. H. C. Torrey, *Phys. Rev.* **76**, 1059 (1949).
17. R. R. Knispel, R. T. Thompson, and M. M. Pintar, *J. Magn. Reson.* **14**, 44 (1974).
18. J. G. Diegel and M. M. Pintar, *Biophys. J.* **15**, 855 (1975).
19. R. Graumann, M. Diemling, T. Heilman, and A. Oppelt, Abstracts of the Society of Magnetic Resonance in Medicine, 5th Annual Meeting, Montreal, p. 992, 1986.
20. Y. T. Zhang, H. N. Yeung, J. Ellis, and P. L. Carson, *Magn. Reson. Med.* **25**, 337 (1992).
21. D. C. Look and D. R. Locker, *Rev. Sci. Instrum.* **41**, 250 (1970).
22. B. M. Fung, *Methods Enzymol.* **127**, 151 (1986).